J|A|C|S
ARTICLES
Published on Web 08/29/2003

Trends in Exchange Coupling for Trimethylenemethane-Type Bis(semiquinone) Biradicals and Correlation of Magnetic Exchange with Mixed Valency for Cross-Conjugated Systems

David A. Shultz,*,§ Rosario M. Fico, Jr.,§ Scot H. Bodnar,§ R. Krishna Kumar,§ Kira E. Vostrikova,§ Jeff W. Kampf,‡ and Paul D. Boyle§

Contribution from the Department of Chemistry, North Carolina State University, Raleigh, North Carolina 27695-8204, and Department of Chemistry, University of Michigan, Ann Arbor, Michigan 48109-1055

Received June 19, 2003; E-mail: david_shultz@ncsu.edu

Abstract: A magnetostructural correlation (conformational electron spin exchange modulation) within an isostructural series of biradical complexes is presented. X-ray crystal structures, variable-temperature electron paramagnetic resonance spectroscopy, zero-field splitting parameters, and variable-temperature magnetic susceptibility measurements were used to evaluate molecular conformation and electron spin exchange coupling in this series of molecules. Our combined results indicate that the ferromagnetic portion of the exchange couplings occurs via the cross-conjugated π-systems, while the antiferromagnetic portion occurs through space and is equivalent to incipient bond formation. Thus, molecular conformation controls the relative amounts of ferro- and antiferromagnetic contributions to exchange coupling. In fact, the exchange parameter correlates with average semiquinone ring torsion angles via a Karplus−Conroy-type relation. Because of the natural connection between electron spin exchange coupling and electronic coupling related to electron transfer, we also correlate the exchange parameters in the biradical complexes to mixed valency in the corresponding quinone−semiquinone radical anions. Our results suggest that delocalization in the cross-conjugated, mixed-valent radical anions is proportional to the *ferromagnetic* contribution to the exchange coupling in the biradical oxidation states.

Introduction

Whether as transient reactive intermediates, as challenging syntheses, as tests of bonding theories, or as objects of theoretical interest, biradicals have held the fascination of chemists for nearly a century.[1−5] Over the past 20 years, biradicals have been studied intensively from a magnetochemistry perspective, with a focus on understanding electron spin exchange coupling. Indeed, some bi- and triradicals have found utility as ligands in the construction of metal ion-containing magnetically ordered solids.[6,7] Chemists now have a thorough understanding of the structural requirements for through-bond electron spin exchange coupling.[8−10] This understanding of exchange coupling allows synthetic chemists to design and prepare new multispin systems with very high-spin ground states.[11,12] In fact, many successful synthetic efforts were preceded by theoretical/computational studies that led to the formation of a rubric for creating high-spin structures.[13−16] This involves attaching spin-containing moieties to a "Coupler" such that the SOMOs in the resulting biradical are "nondisjoint" (biradical obeys Hund's first rule).[14] Several saturated and π-system Couplers have been identified and explored.[8,9]

To fully reveal the relationships between molecular structure and ferromagnetic exchange coupling, one must understand the effects of both substituents and conformation.[17−19] We recently presented the first experimental examples of substituent-modulated exchange coupling in a series of triplet ground-state biradicals **1(SQZnL)$_2$** (Scheme 1),[20] As for conformation-dependent exchange coupling, it has been understood for some

§ North Carolina State University.
‡ University of Michigan.

(1) Chichibabin, A. E. *Ber. Dtsch. Chem. Ges.* **1907**, *40*, 1810−1819.
(2) Schlenk, W.; Brauns, M. *Chem. Ber.* **1915**, *48*, 661−669.
(3) Schlenk, W.; Brauns, M. *Chem. Ber.* **1915**, *48*, 716−728.
(4) Wentrup, C. *Science* **2002**, *295*, 1846−1847.
(5) Scheschkewitz, D.; Amii, H.; Gornitzka, H.; Schoeller, W. W.; Bourissou, D.; Bertrand, G. *Science* **2002**, *295*, 1880−1881.
(6) Iwamura, H.; Inoue, K.; Haymizu, T. *Pure Appl. Chem.* **1996**, *68*, 243−252.
(7) Inoue, K.; Hayamizu, T.; Iwamura, H.; Hashizume, D.; Ohashi, Y. *J. Am. Chem. Soc.* **1996**, *118*, 1803−1804.
(8) Dougherty, D. A. *Acc. Chem. Res.* **1991**, *24*, 88−94.
(9) Rajca, A. *Chem. Rev.* **1994**, *94*, 871−893.
(10) Lahti, P. M. *Magnetic Properties of Organic Materials*; Marcel Dekker: New York, 1999.
(11) Rajca, A.; Wongsriratanakul, J.; Rajca, S. *Science* **2001**, *294*, 1503−1505.
(12) Rajca, A.; Rajca, S.; Wongsriratanakul, J. *J. Am. Chem. Soc.* **1999**, *121*, 6308−6309.
(13) Jacobs, S. J.; Shultz, D. A.; Jain, R.; Novak, J.; Dougherty, D. A. *J. Am. Chem. Soc.* **1993**, *115*, 1744−1753.
(14) Borden, W. T.; Davidson, E. R. *J. Am. Chem. Soc.* **1977**, *99*, 4587−4594.
(15) Borden, W. T. *Diradicals*; Wiley: New York, 1982.
(16) Borden, W. T.; Iwamura, H.; Berson, J. A. *Acc. Chem. Res.* **1994**, *27*, 109−116.
(17) For work on substituent and conformation effects on biradicals using computational chemistry and EPR spectroscopy, see the following and ref 18: Silverman, S. K.; Dougherty, D. A. *J. Phys. Chem.* **1993**, *97*, 13273−13283.
(18) West, A. P., Jr.; Silverman, S. K.; Dougherty, D. A. *J. Am. Chem. Soc.* **1996**, *118*, 1452−1463.
(19) For electronic modulation of ***J*** for singlet ground-state biradicals, see: Berson, J. A. Structural Determinants of the Chemical and Magnetic Properties of Non-Kekule Molecules. In *Magnetic Properties of Organic Materials*; Lahti, P. M., Ed.; Marcel Dekker: New York, 1999; pp 7−26.

Scheme 1

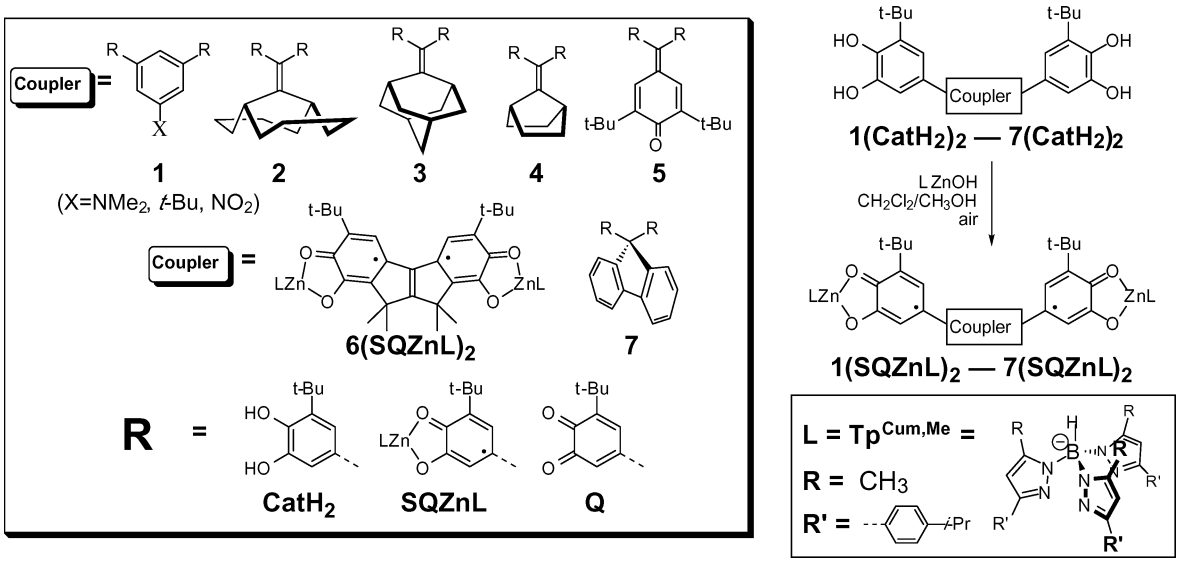

Scheme 2

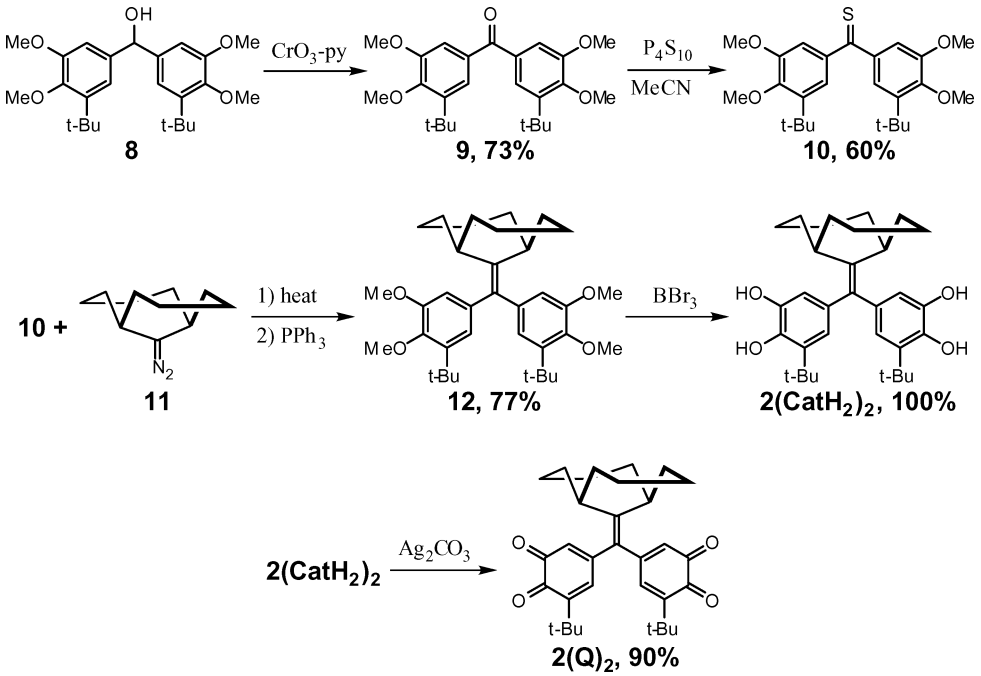

time that severe torsions of bonds that connect spin-containing and Coupler fragments attenuate exchange coupling, albeit not in an isostructural series, rather in a handful of disparate examples.[21] Herein, we report the first magnetostructural study of conformational exchange modulation in an isostructural series of bis(semiquinone) complexes.

Furthermore, we show how energy matching of Coupler and semiquinone (SQ) orbitals can enhance exchange coupling. Finally, because of the natural connection between electron spin exchange coupling and electronic coupling matrix elements pertinent to electron transfer, we correlate magnetic exchange coupling with Coupler-modulated delocalization within mixed-valent forms of our ligands.

Results and Analysis

Synthesis. The biradical complexes **2(SQZnL)$_2$**−**7(SQZnL)$_2$** presented here are shown in Scheme 1, left (R = **SQZnL**). Complex formation generally follows a procedure (Scheme 1, right) reported previously by Pierpont,[22] and adopted by us (see Experimental Section for details). The bis(catechol) ligands, **3-(CatH$_2$)$_2$**−**7(CatH$_2$)$_2$** have been reported previously,[23,24] except for **2(CatH$_2$)$_2$**. The synthetic outline for preparation of new molecules is given in Scheme 2.

Preparation of **2(CatH$_2$)$_2$** begins with carbinol **8**[24] which was oxidized to ketone **9** and subsequently transformed into thione **10** using P_4S_{10}.[25] Reaction of thione **10** with diazo compound

(20) Shultz, D. A.; Bodnar, S. H.; Lee, H.; Kampf, J. W.; Incarvito, C. D.; Rheingold, A. L. *J. Am. Chem. Soc.* **2002**, *124*, 10054−10061.
(21) Shultz, D. A. Conformational Exchange Modulation in Trimethylenemethane (TMM)-Type Biradicals. In *Magnetic Properties of Organic Materials*; Lahti, P., Ed.; Marcel Dekker: New York, 1999.
(22) Ruf, M.; Noll, B. C.; Groner, M. D.; Yee, G. T.; Pierpont, C. G. *Inorg. Chem.* **1997**, *36*, 4860−4865.
(23) Shultz, D. A.; Boal, A. K.; Lee, H.; Farmer, G. T. *J. Org. Chem.* **1998**, *63*, 9462−9469.
(24) Shultz, D. A.; Lee, H.; Fico, R. M., Jr. *Tetrahedron* **1999**, *55*, 12079−12086.

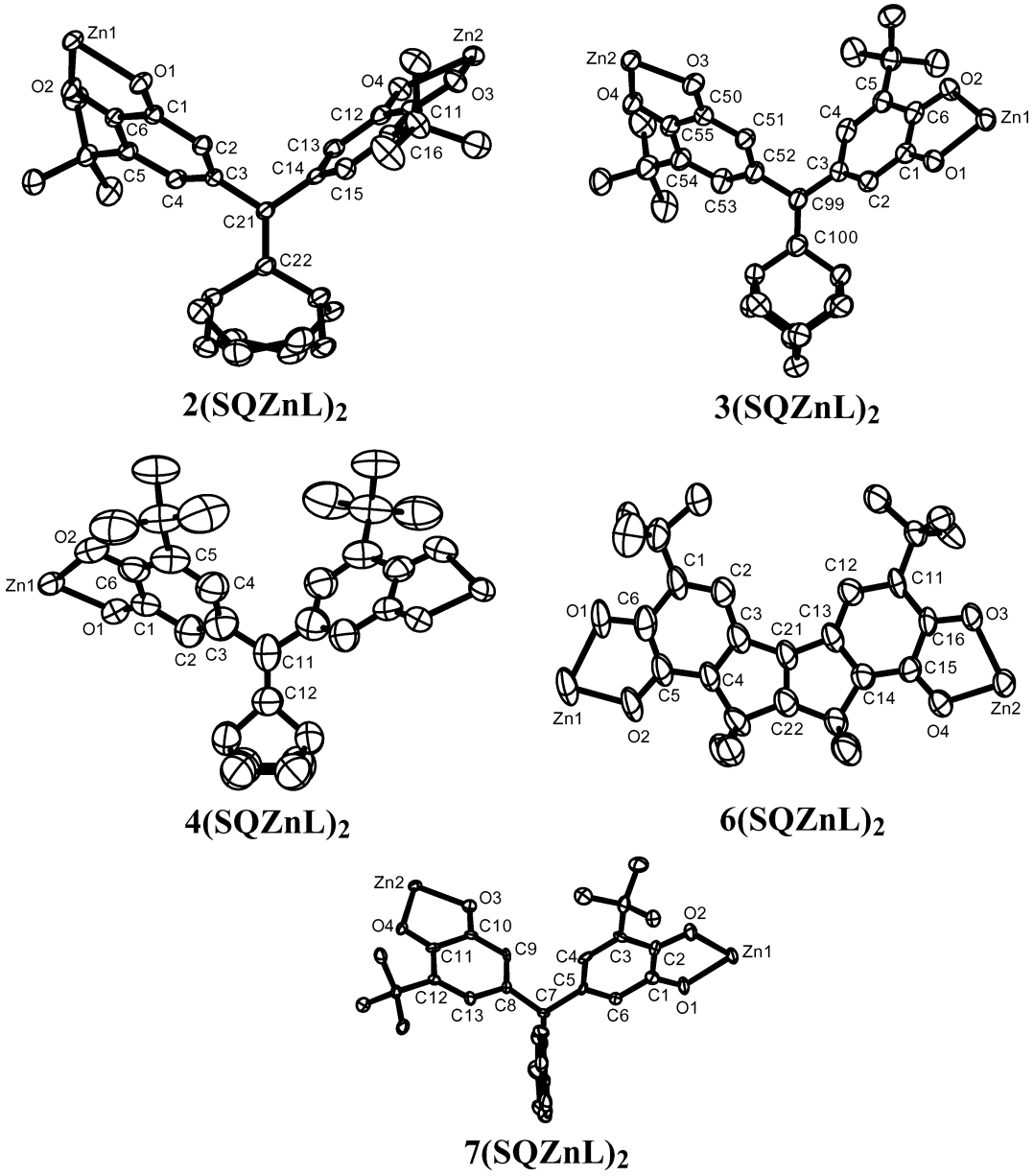

Figure 1. Thermal ellipsoid plots of **2(SQZnL)$_2$**−**4(SQZnL)$_2$**, **6(SQZnL)$_2$**, and **7(SQZnL)$_2$**. Ancillary ligands and hydrogens have been omitted for clarity.

11,[26] followed by desulfurization with triphenylphosphine gave alkene **12**. Deprotection afforded **2(CatH$_2$)$_2$**, and oxidation gave bis(quinone) **2(Q)$_2$**.

Molecular Structures and Conformations. The molecular structures of **2(SQZnL)$_2$**−**7(SQZnL)$_2$** were determined by X-ray crystallography, and thermal ellipsoid plots are shown in Figure 1. The structure of **5(SQZnL)$_2$** was reported previously.[27] Important structural parameters are collected in Tables 1 and 2. All of the dioxolene bond lengths are consistent with the SQ oxidation state as opposed to Cat or CatH.[28−30] Other bond lengths and angles are listed in the Supporting Information.

Frozen-Solution EPR Spectroscopy. Figure 2 shows the EPR spectra of **2(SQZnL)$_2$**−**7(SQZnL)$_2$** recorded at 77 K in 2-MTHF. All spectra are consistent with randomly oriented triplet species[31] along with small amounts of doublet monoradical impurities.[32] The zero-field-splitting parameters for the biradicals, obtained by simulation,[33] are given in Table 3. The spectral shapes of all biradicals, except **3(SQZnL)$_2$**, are invariant with temperature changes (4−77 K), suggesting the absence of rotamers.[34] The results for **3(SQZnL)$_2$** are discussed below.

Variable-Temperature EPR Spectroscopy. Curie plots for the doubly integrated $\Delta m_s = 2$ signals of **2(SQZnL)$_2$**−**7-**

(25) Scheeren, J. W.; Ooms, P. H. J.; Nivard, R. J. F. *Synthesis* **1973**, 149−151.
(26) Shultz, D. A.; Boal, A. K.; Lee, H.; Farmer, G. T. *J. Org. Chem.* **1999**, *64*, 4386-4396.
(27) Shultz, D. A.; Bodnar, S. H.; Kampf, J. W. *Chem. Commun.* **2001**, 93−94.
(28) Pierpont, C. G.; Lange, C. W. *Prog. Inorg. Chem.* **1994**, *41*, 331−442.
(29) Ruf, M.; Lawrence, A. M.; Noll, B. C.; Pierpont, C. G. *Inorg. Chem.* **1998**, *37*, 1992−1999.
(30) Shultz, D. A.; Bodnar, S. H.; Kumar, R. K.; Lee, H.; Kampf, J. W. *Inorg. Chem.* **2001**, *40*, 546−549.
(31) Wasserman, E.; Snyder, L. C.; Yager, W. A. *J. Chem. Phys.* **1964**, *41*, 1763−1772.
(32) Some of the $g = 2$ signal is a double-quantum transition as shown by power dependence studies, see: deGroot, M. S.; van der Waals, J. H. *Physica* **1963**, *29*, 1128−1132.
(33) Bruker *WINEPR SimFonia*, 1.25, Shareware Version ed.; Brüker Analytische Messtechnik GmbH: Karlsruhe, Germany, 1996.
(34) Shultz, D. A.; Boal, A. K.; Farmer, G. T. *J. Am. Chem. Soc.* **1997**, *119*, 3846−3847.

Table 1. Important Bond Lengths

Biradical	Bond	Length (Å)	Bond	Length (Å)
2(SQZnL)$_2$ [semiquinone rings]	C1-O1	1.288(4)	C12-O4	1.286(4)
	C1-C6	1.488(5)	C12-C11	1.469(5)
	C6-O2	1.273(4)	C11-O3	1.271(4)
	C6-C5	1.441(5)	C11-C16	1.446(5)
	C5-C4	1.367(5)	C16-C15	1.371(5)
	C4-C3	1.446(5)	C15-C14	1.440(5)
	C3-C2	1.372(5)	C14-C13	1.356(5)
	C2-C1	1.400(5)	C13-C12	1.414(5)
[SQ-ethene] C=C	C3-C21	1.496(5)	C14-C21	1.503(5)
	C21-C22	1.356(5)		
3(SQZnL)$_2$ [semiquinone rings]	C50-O3	1.290(7)	C1-O1	1.293(6)
	C50-C55	1.474(8)	C1-C6	1.462(8)
	C55-O4	1.283(6)	C6-O2	1.278(7)
	C55-C54	1.441(8)	C6-C5	1.455(8)
	C54-C53	1.367(8)	C5-C4	1.374(8)
	C53-C52	1.437(8)	C4-C3	1.439(8)
	C52-C51	1.386(8)	C3-C2	1.376(8)
	C51-C50	1.397(8)	C2-C1	1.400(8)
[SQ-ethene] C=C	C52-C99	1.497(8)	C3-C99	1.474(8)
	C99-C100	1.355(8)		
4(SQZnL)$_2$ [semiquinone rings]	C1-O1	1.261(9)		
	C1-C2	1.416(11)		
	C1-C6	1.461(12)		
	C2-C3	1.351(12)		
	C3-C4	1.409(13)		
	C4-C5	1.393(13)		
	C5-C6	1.466(13)		
	C6-O2	1.281(10)		
[SQ-ethene] C=C	C3-C11	1.500(13)		
	C11-C12	1.343(19)		
6(SQZnL)$_2$ [semiquinone rings]	O1-C1	1.282(9)	O3-C11	1.294(11)
	O2-C2	1.323(10)	O4-C12	1.324(11)
	C1-C6	1.430(12)	C11-C12	1.441(15)
	C1-C2	1.469(12)	C11-C16	1.481(14)
	C2-C3	1.375(12)	C12-C13	1.384(13)
	C3-C4	1.422(13)	C13-C14	1.389(12)
	C4-C5	1.412(12)	C14-C15	1.416(14)
	C5-C6	1.361(12)	C15-C16	1.360(13)
[SQ-ethene] C=C	C4-C21	1.421(12)	C14-C21	1.476(13)
	C21-C22	1.362(13)		
7(SQZnL)$_2$ [semiquinone rings]	C10-O3	1.285(9)	C1-O1	1.304(10)
	C10-C11	1.485(12)	C1-C2	1.437(12)
	C11-O4	1.277(10)	C2-O2	1.314(10)
	C11-C12	1.429(11)	C2-C3	1.442(12)
	C12-C13	1.371(11)	C3-C4	1.378(12)
	C13-C8	1.428(11)	C4-C5	1.420(13)
	C8-C9	1.368(12)	C5-C6	1.376(11)
	C9-C10	1.406(11)	C6-C1	1.420(12)
[SQ-fluorene]	C8-C7	1.521(11)	C5-C7	1.555(11)

Table 2. Semiquinone Ring Torsion Angles[a–d]

biradical	semiquinone ring torsion angles (deg)[a]	average semiquinone ring torsion angles (deg)
2(SQZnL)$_2$	64.10 ± 0.13, 78.04 ± 0.13	71.1 ± 3.5
3(SQZnL)$_2$	47.51 ± 0.18, 48.94 ± 0.27	48.23 ± 0.4
4(SQZnL)$_2$	48.37 ± 0.29	48.37±0.29
5(SQZnL)$_2$[b]	50.3 ± 0.3, 42.6 ± 0.8	46.5 ± 3.9
6(SQZnL)$_2$	4.9 ± 0.8, 9.7 ± 0.8	7.3 ± 2.4
7(SQZnL)$_2$	42.3 ± 0.9, 52.4 ± 0.1	47.4 ± 2.5

[a] Torsion angle defined as the angle between the plane of a SQ ring and the plane containing the ethene Coupler. [b] Data from ref 27. [c] **7(SQZnL)$_2$** torsion angles defined as bond torsion through the sp^3 carbon of the fluorenyl group.

(SQZnL)$_2$ are shown in Figure 3, and are summarized in Table 4. Biradicals **4(SQZnL)$_2$**−**7(SQZnL)$_2$** gave linear responses, consistent with $J > 0$ (ferromagnetic coupling) or $J = 0$,[35] and are in agreement with our previous findings on bis(SQ)s prepared by electrochemical and chemical reduction.[23,24] The intensity of $\Delta m_s = 2$ signal of **2(SQZnL)$_2$** varies with decreasing temperature consistent with antiferromagnetic coupling. The data were fit to eq 1:[35]

$$I_{EPR} = \frac{C}{T}\left[\frac{3\exp\left(\frac{-2J}{kT}\right)}{1+3\exp\left(\frac{-2J}{kT}\right)}\right] \quad (1)$$

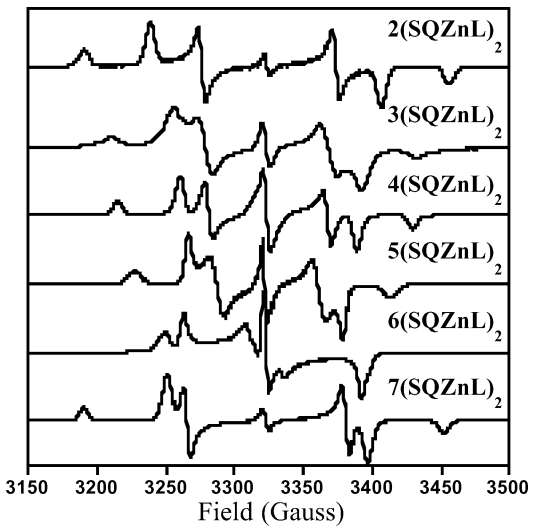

Figure 2. EPR spectra of biradicals **2(SQZnL)$_2$**−**7(SQZnL)$_2$** collected at 77 K in 2-MTHF.

where C is a constant and J is the exchange parameter. Best fit results give $J = -35$ cm^{-1}.

(35) Berson, J. A. *The Chemistry of the Quinonoid Compounds*; Patai, S. R., Z., Ed.; John Wiley & Sons: New York, 1988; Vol. II, p 482.

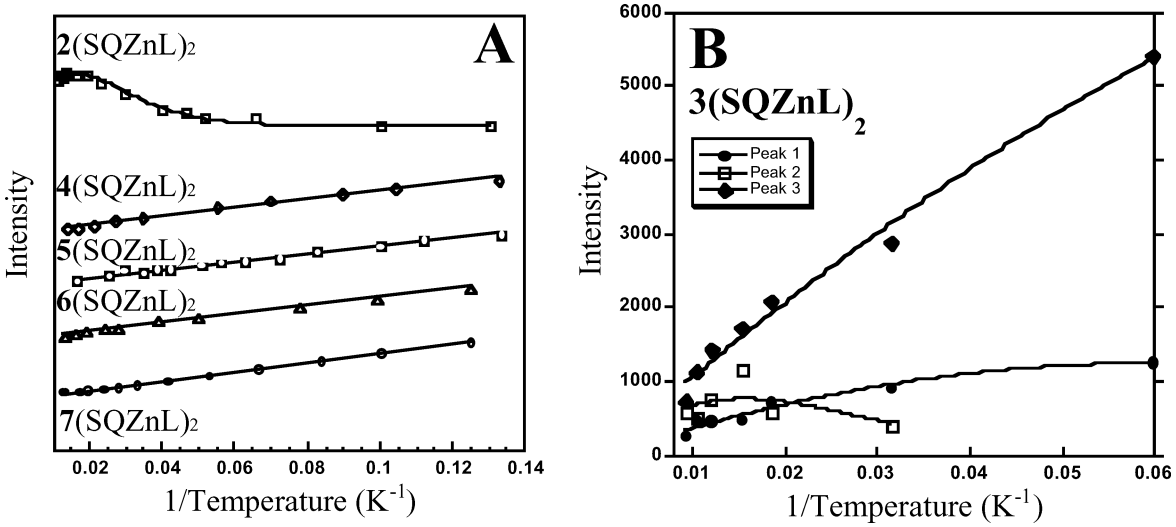

Figure 3. EPR Curie plots for biradical complexes **2(SQZnL)$_2$**, **4(SQZnL)$_2$**−**7(SQZnL)$_2$** (A) and **3(SQZnL)$_2$** (B).

Table 3. Zero-Field-Splitting Parameters

biradical	$\|D/hc\|$ (cm^{-1})	$\|E/hc\|$ (cm^{-1})	$\|E/D\|$
2(SQZnL)$_2$	0.0124	0.0011	0.0887
3(SQZnL)$_2$	0.0105	0.0008	0.0762
4(SQZnL)$_2$	0.0098	0.0006	0.0612
5(SQZnL)$_2$	0.0093	0.0006	0.0645
6(SQZnL)$_2$	0.0068	0.0017	0.2500
7(SQZnL)$_2$	0.0123	0.0005	0.0407

Table 4. Variable-Temperature Susceptibility Fit Parameters, and Results from Variable-Temperature EPR Experiments[a]

biradical	J (cm^{-1})[b]	zJ' (cm^{-1})[c]	EPR Curie plot, J(cm^{-1})
2(SQZnL)$_2$	-30.3 ± 0.8[d]	$+0.011 \pm 0.001$	curved, −35
3(SQZnL)$_2$	$+24.4 \pm 0.6$	-0.032 ± 0.008	curved, −3,−9,−38
4(SQZnL)$_2$	$+87.0 \pm 3.0$	-0.024 ± 0.018	linear, $J \geq 0$
5(SQZnL)$_2$[e]	$+209.4 \pm 1.4$	-0.029 ± 0.002	linear, $J \geq 0$
6(SQZnL)$_2$	$+163.6 \pm 1.6$	-0.080 ± 0.004	linear, $J \geq 0$
7(SQZnL)$_2$	$+0.99 \pm 0.06$	-0.503 ± 0.021	linear, $J \geq 0$

[a] Fits used $g = 2.002$. [b] $J > 0$ for triplet ground-state. [c] Intermolecular interaction. [d] J-value for average determined from χ_{para} vs T plot fit parameters and T_{max}. [e] Fit parameters from from ref 27.

The $\Delta m_s = 1$ region of the EPR spectrum of biradical **3-(SQZnL)$_2$** shows that at least three rotamers characterized by different zero-field splitting parameters are present (see Supporting Information). By fitting either the intensities of the low-field z-transition of the $\Delta m_s = 1$ region, or by fitting the doubly integrated $\Delta m_s = 2$ region to eq 1, we find best fits for three rotamers having $J \approx -3$, -9, and -38 cm^{-1}. This result differs from the linear Curie plot for the sodium salt of the **3(SQ)$_2$**,[36] but parallels the results for the corresponding bis(phenoxy) radical.[34]

Solid-State Magnetic Susceptibility Measurements. The magnetic susceptibility data for all of the compounds are plotted in Figure 4. Modeling the temperature-dependent $\chi_{para}T$ products of $S = 1$ molecules can be achieved by fitting to a field-independent van Vleck expression, eq 2,[37,38]

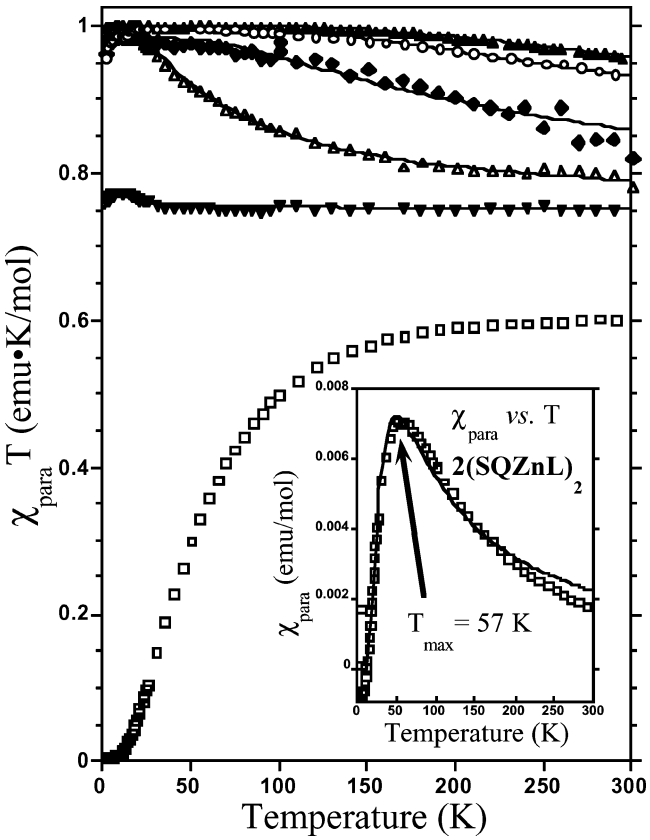

Figure 4. $\chi_{para}T$ vs T plots: **2(SQZnL)$_2$** (□); **3(SQZnL)$_2$** (△); **4(SQZnL)$_2$** (◆); **5(SQZnL)$_2$** (▲); **6(SQZnL)$_2$** (○); **7(SQZnL)$_2$** (▼). Inset: χ_{para} vs T plot for **2(SQZnL)$_2$**.

$$\chi T = \frac{2Ng^2\beta^2}{k[3 + e^{-2J/kT}]} \qquad (2)$$

where g is the isotropic Landé constant ($g = 2.0023$), β is the Bohr magneton, T is temperature in Kelvin, k is Boltzmann's constant, and J is the intramolecular SQ−SQ exchange coupling parameter. The relative singlet- and triplet-state energies were derived using the Hamiltonian, $H = -2J\hat{S}_1 \cdot \hat{S}_2$, where $\hat{S}_1$ and $\hat{S}_2$ are the spin operators for the SQs. The decrease in the χT data at low temperatures was accounted for with a Weiss correction, using the expression $\chi_{eff} = \chi/(1 - \vartheta\chi)$, where $\vartheta =$

(36) Shultz, D. A.; Boal, A. K.; Driscoll, D. J.; Farmer, G. T.; Hollomon, M. G.; Kitchin, J. R.; Miller, D. B.; Tew, G. N. *Mol. Cryst. Liq. Cryst.* **1997**, *305*, 303−310.
(37) Kahn, O. *Molecular Magnetism*; VCH: New York, 1993; p 104.
(38) Bleaney, B.; Bowers, K. D. *Proc. R. Soc. London* **1952**, *A214*, 451−465.

Table 5. Cyclic Voltammetric Data for Bis(quinones)[a]

bis(quinone)	$E_{1/2}$(1)[b]	$E_{1/2}$(2)[c]	$\Delta E_{1/2}$[d]	K_{com}[e]
2(Q)$_2$	−0.81	−1.00	−0.19	1625
3(Q)$_2$	−0.83	−1.04	−0.21	3540
4(Q)$_2$	−0.77	−0.99	−0.22	5225
5(Q)$_2$	−0.60	−0.85	−0.25	16 790
6(Q)$_2$	−0.82	−1.09	−0.27	36 560
7(Q)$_2$	−0.81	−1.01	−0.20	2400

[a] 0.5 mM bis(quinone) in THF, 100 mM *n*-Bu_4NPF_6 electrolyte; potentials in volts vs ferrocene; scan rate = 200 mV/s; data for **2(Q)$_2$**−**7(Q)$_2$** from ref 23. [b] Redox potential for bis(Q)/(Q−SQ) couple; $E_{1/2} = (E_{p,c} - E_{p,a})/2$. [c] Redox potential for (Q−SQ)/bis(SQ) couple; $E_{1/2} = (E_{p,c} - E_{p,a})/2$. [d] $\Delta E_{1/2} = E_{1/2}(2) - E_{1/2}(1)$. [e] $\log K_{com} = 16.9\Delta E_{1/2}$.

$2zJ'/(Ng^2\beta^2)$.[39] The origin of zJ' may be zero-field splitting, intermolecular interaction, saturation effects, or some combination of all three.[40] The other terms have their usual meanings.[39] All curve fit results are presented in Table 4.

The results for **2(SQZnL)$_2$** are displayed as a χ_{para} vs T plot as the inset in Figure 4. For antiferromagnetically coupled dimers, the χ_{para} vs T plot displays a signature maximum with $T_{max} = 1.285\ J/k$.[37] We were unable to satisfactorily fit the low-temperature region of either the $\chi_{para}T$ or χ_{para} vs T plot. Nevertheless, the J-value from the fit parameters ($-29.5\ cm^{-1}$) compares well with the value of J determined from T_{max} ($J = -31\ cm^{-1}$). The value for $\boldsymbol{J}$ given in Table 4 represents an average of the values from the fit and from the value determined from T_{max}.

Electrochemistry of Corresponding Bis(Quinone)s. The cyclic voltammograms of **3(Q)$_2$**−**7(Q)$_2$** have been presented previously.[23,24] It was noted that the separation of the first and second redox processes (corresponding to reversible production of the mixed-valent quinone/SQ and isovalent bis(SQ)s) followed a periodic trend. Pertinent data are reproduced in Table 5 along with new data for **2(Q)$_2$**. The difference in the first and second redox potentials ($\Delta E_{1/2}$) can be used to calculate the equilibrium constant for the comproportionation reaction, eq 3.[41] Thus, K_{com} is a measure of the stability of the mixed-valent semiquione-quinone (Q−SQ) species.[41]

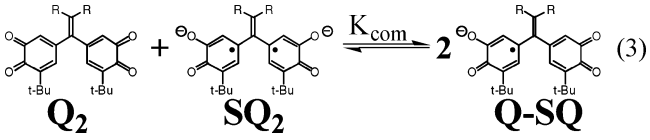

(3)

Discussion

Biradical Design Elements, Molecular Structures, and Conformations. Design elements of a generic trimethylenemethane-type (TMM-type)[23] biradical have been presented previously.[26] These design elements are featured in our series of bis(SQ) complexes. The π-systems are cross-conjugated and therefore fulfill the π-connectivity requirements for ferromagnetic coupling of the unpaired electrons of the SQ spin-containing units.[14] "Capping groups" provide steric protection of the delocalized unpaired electrons. It is the steric interactions between atoms in the capping group and those in the spin-containing unit that disrupt conjugation between the spin-containing units and the TMM functionality to provide conformational modulation of exchange coupling.[21]

Possible capping groups include aryl groups and bicyclic or tricyclic ring systems. Simple primary or secondary alkyl groups were not considered since they contain allylic hydrogens that are excellent candidates for abstraction and subsequent loss of spin.[42] However, the bridgehead C−H bonds of bicyclic or tricyclic ring-capping groups are orthogonal to the ethene Coupler π-bond. Moreover, these bridgehead hydrogens experience van der Waals repulsions with the SQ rings when the SQs approach coplanarity with the ethene Coupler. This steric interaction will result in conformational attenuation of ferromagnetic exchange coupling and should increase as the bond angle θ increases. The success of this approach was first seen in a series of isostructural dinitroxide biradicals reported previously.[26] In the present case, control over biradical conformation for the bis(SQ)s via the capping group can be seen in the SQ ring torsion angles relative to the ethene Couplers determined by X-ray crystallographic analysis (Table 2). Generally, the SQ ring torsion angles increase in going from **6(SQZnL)$_2$** (in which the conformation is held nearly planar by covalent bonds) to **2(SQZnL)$_2$**. The similarity in the conformations of **3(SQZnL)$_2$** and **4(SQZnL)$_2$** was unexpected, as molecular mechanics predicted a ca. 10° difference in SQ ring torsions.[26] Nevertheless, a range of SQ ring torsions in biradicals having the same Coupler is achieved.

As mentioned in the previous section, all dioxolene bond lengths are in accord with the SQ oxidation state. Small deviations from "standard"[22] lengths are common for SQs with conjugating substituents.[27,43] In addition, the C═C Coupler bond lengths for **2(SQZnL)$_2$**−**4(SQZnL)$_2$** and **6(SQZnL)$_2$** are also within the range of C═C bond lengths for 1,1-diaryl-, triaryl-, and tetraarylethenes (1.343 ± 0.14 Å) gleaned from the Cambridge Structural Database.[44]

Zero-Field Splitting Parameters as a Measure of Biradical Electronic Structure and Conformation. Because the mechanism for zero-field splitting (zfs) in organic biradicals is dipolar, zfs parameters (D and E) strongly correlate with molecular conformation.[45−48] Such is the case for **2(SQZnL)$_2$**−**7(SQZnL)$_2$**: D and E are consistent with both their electronic structures[23,24] and D is a direct measure of the SQ ring torsions.[49−51] As can be seen in Figure 2, $|D/hc|$ decreases in the series **2(SQZnL)$_2$**−**7(SQZnL)$_2$** consistent with the corresponding decrease in SQ ring torsions as suggested in Figure 5. Since the trend in experimental zfs parameters is consistent with the conformations determined by the crystal structures, we conclude that the conformations observed in the solid state are similar to those in frozen solution. Our contention is supported

(39) O'Connor, C. J. *Prog. Inorg. Chem.* **1982**, *29*, 203−283.
(40) Caneschi, A.; Dei, A.; Mussari, C. P.; Shultz, D. A.; Sorace, L.; Vostrikova, K. E. *Inorg. Chem.* **2002**, *41*, 1086−1092.
(41) Ward, M. D. *Chem. Soc. Rev.* **1995**, *24*, 121−134.
(42) Anderson, K. K.; Shultz, D. A.; Dougherty, D. A. *J. Org. Chem.* **1997**, *62*, 7575−7584.
(43) Shultz, D. A.; Bodnar, S. H.; Kumar, R. K.; Kampf, J. W. *J. Am. Chem. Soc.* **1999**, *121*, 10664−10665.
(44) Allen, F. H. *Acta Crystallogr.* **2002**, *B58*, 380−388.
(45) Ullman, E. F.; Boocock, D. G. B. *J. Chem. Soc., Chem. Commun.* **1969**, *20*, 1161−1162.
(46) Mukai, K.; Tamaki, T. *Bull. Chem. Soc. Jpn.* **1977**, *50*, 1239−1244.
(47) Sandberg, K. A.; Shultz, D. A. *J. Phys. Org. Chem.* **1998**, *11*, 819−824.
(48) We were unsuccessful at calculating the zfs parameters for our biradicals using the methods described in ref 47, possibly due to the fact several of the biradicals are between the extremes of disjoint and nondisjoint.
(49) For beautiful examples of $|D/hc|$ as a measure of delocalization, see the following plus refs 50 and 51: Jain, R.; Sponsler, M. B.; Coms, F. D.; Dougherty, D. A. *J. Am. Chem. Soc.* **1988**, *110*, 1356−1366.
(50) Rajca, A.; Utamapanya, S.; Xu, J. *J. Am. Chem. Soc.* **1991**, *113*, 9235−9241.
(51) Rajca, A.; Utamapanya, S. *J. Org. Chem.* **1992**, *57*, 1760−1767.

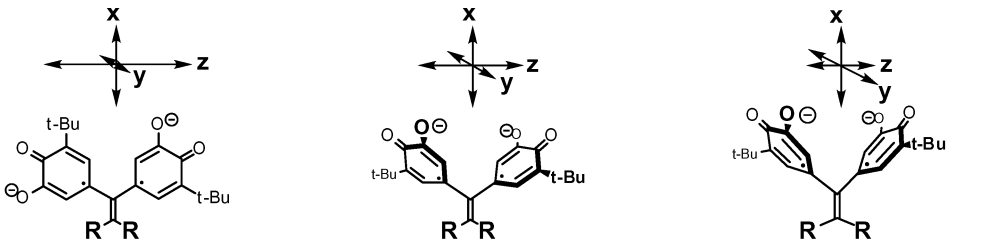

Figure 5. How conformation manifests itself in the zero-field splitting parameters. Axes are for illustration purposes only, and are not meant necessarily to represent principal axes of the *D* tensor.

by the similarity of the solution- and solid-state *J*-parameters for **2(SQZnL)$_2$** (Table 4). Moreover, we conclude that severe torsions of the SQ rings (e.g., **2(SQZnL)$_2$**) cause the unpaired electrons of the SQ π-systems to be "stacked" in such a way to favor incipient σ-bond formation.[52,53] Thus, the same structural features that give rise to large $|D/hc|$ as indicated in Figure 5, also result in increased antiferromagnetic coupling in TMM-type biradicals.

We also note that **3(SQZnL)$_2$** exhibits multiple EPR signals as a function of temperature (see Supporting Information for spectra) that are consistent with different rotamers having different exchange parameters, *J* (Figure 3B). Similar behavior was observed by us for the phenoxy biradical analogue of **3-(SQZnL)$_2$**,[34] and the nitroxide analogue of **3(SQZnL)$_2$** undergoes a hysteretic transition involving molecular conformation.[54] It appears that the adamantyl Capping group results in shallow conformational potential energy surface for 1,1-diarylethenes that can accommodate several metastable conformations.

The Nature of the Exchange Couplings. The exchange coupling parameter, *J*, is a sum of ferromagnetic and antiferromagnetic terms. As shown in eq 4, the ferromagnetic term (J_F) is composed of the exchange integral, *k* (the electron−electron repulsion in the overlap region: $k = \langle\phi_1(1)\phi_2(1)|e^2/r_{12}|\phi_1(2)\phi_2(2)\rangle$, where $\phi_1(1)\phi_2(1)$ is the overlap density), while the antiferromagnetic term (J_{AF}) is the result of configuration interaction that arises from mixing of two singlet states via transfer (resonance) integral β, and separated by energy *U*.[37,55,56] The integral *l* is the hybrid coulomb integral, and represents the electron−electron repulsion between an electron in an orbital with one in the overlap region (e.g., $l = \langle\phi_1(1)\phi_2(1)|e^2/r_{12}|\phi_2(2)\phi_2(2)\rangle$, where $\phi_1(1)\phi_2(1)$ represents the overlap density).[37,57]

$$J = J_F + J_{AF} \approx 2k - \frac{4(\beta + l)^2}{U} \qquad (4)$$

The cross-conjugated π-connectivity of our biradicals ensures nondisjoint SOMOs,[14] and therefore a sizable exchange integral such that in the absence of severe bond torsions,[21] the triplet state is lower in energy than the singlet state. Perusal of Table 4 shows this to be the case: in the solid state, all of the biradicals save **2(SQZnL)$_2$** are triplet ground-state species but increased SQ ring torsions make *J* less ferromagnetic (or more antiferromagnetic). Severe twisting, as in **2(SQZnL)$_2$**, gives rise to a singlet ground-state biradical.

The molecular conformation of **5(SQZnL)$_2$** is similar to that of **3(SQZnL)$_2$** and **4(SQZnL)$_2$**, yet the exchange parameter is significantly greater for **5(SQZnL)$_2$** than for the latter two. We hypothesize that the orbitals of the quinone−methide Coupler of **5(SQZnL)$_2$** mix more effectively with those of the SQ groups than do those of a simple ethene Coupler. Our hypothesis is supported by the fact that the **5(Q)$_2$** ⇔ **5(SQ)$_2$** redox couples are more positive than those of the corresponding couples for molecules with a simple C═C Coupler (see Table 5). The more positive redox potentials suggest that the redox orbitals are lower in energy by virtue of stronger mixing with quinone−methide (Coupler) orbitals. The result of this stronger mixing is greater overlap density which in a biradical oxidation state implies a larger exchange integral. This result parallels the findings for bridge substitution in donor−acceptor molecular wires.[58]

The exchange parameter for the fluorenyl-linked biradical **7-(SQZnL)$_2$** is also noteworthy. This biradical is comprised of two SQs linked in a geminal fashion to an sp^3 carbon and therefore gives us the opportunity to determine the overall effectiveness of the C═C Coupler. As can be seen from the meager *J*-parameter of **7(SQZnL)$_2$** compared to that of **4-(SQZnL)$_2$** or to that of **6(SQZnL)$_2$**, the C═C Coupler is indeed more effective at promoting ferromagnetic exchange coupling than an sp^3 carbon.[59]

How does one evaluate the antiferromagnetic contributions to the exchange parameter in this series? Nominally, our TMM-type bis(SQ)s **2(SQZnL)$_2$**−**7(SQZnL)$_2$** have C_2 symmetry[60] and the two Hückel SOMOs transform as *a* and *b* irreducible representations as shown in Figure 6.

The electronic configurations (a^1b^1), (a^2b^0), and (a^0b^2) form four low-lying electronic states: two open-shell states, ^{3}B and ^{1}B, and two zwitterionic ^{1}A states, respectively. At this symmetry, configuration interaction cannot provide an antiferromagnetic contribution to the exchange parameter since the lowest singlet is B and the zwitterionic singlets are A. Therefore,

(52) Hatfield, W. E. Chapter 7. Properties of Condensed Compounds (Compounds with Spin Exchange). In *Theory and Applications of Molecular Paramagnetism*; Boudreaux, E. A., Mulay, L. N., Eds.; Wiley-Interscience: New York, 1976; pp 381−385.
(53) Anderson, P. W. *Phys. Rev.* **1959**, *115*, 2−13.
(54) Shultz, D. A.; Fico, R. M., Jr.; Boyle, P. D.; Kampf, J. W. *J. Am. Chem. Soc.* **2001**, *123*, 10403−10404.
(55) Hay, P. J.; Thibeault, J. C.; Hoffmann, R. *J. Am. Chem. Soc.* **1975**, *97*, 4884−4899.
(56) Kahn, O.; Briat, B. *J. Chem. Soc., Faraday Trans. 2* **1976**, *72*, 268−281.
(57) Michl, J.; Bonacic-Koutecky, V. *Electronic Aspects of Organic Photochemistry*; Wiley-Interscience: New York, 1990.
(58) Davis, W. B.; Svec, W. A.; Ratner, M. A.; Wasielewski, M. R. *Nature* **1998**, *396*, 60−63.
(59) Goldberg, A. H.; Dougherty, D. A. *J. Am. Chem. Soc.* **1983**, *105*, 284−290.
(60) C_{2v} symmetry is precluded by steric interactions between the SQ groups.

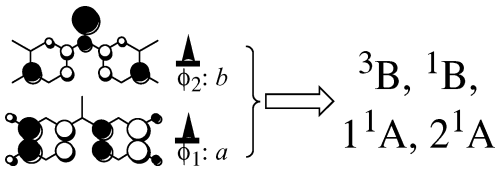

Figure 6. TMM-type bis(SQ) Hückel SOMOs (triplet electronic configuration shown) and electronic states.

^{1}B and ^{1}A can mix only through *b* vibrations.[61] That is to say J_{AF} is vibronic.[62] Moreover, if it is true generally that vibronic coupling matrix elements are smaller than configuration interaction matrix elements, then C_2-symmetric biradicals are less likely to have singlet ground states since J_{AF} is attenuated compared to a higher-symmetry case where configuration interaction contributes to J_{AF}. Of course, configuration interaction will operate when orbitals other than those that are singly occupied are involved.

The preceding discussion notwithstanding, the crystal structures of **2(SQZnL)$_2$**−**7(SQZnL)$_2$** show that the molecules in the solid-state are asymmetric.[63] As such, configuration interaction *will* contribute to J_{AF}. However, there is another antiferromagnetic contribution: direct through-space interaction of SQ groups. This contribution results from the close spatial proximity of the *geminal* SQ groups (see also EPR section above) and is equivalent to incipient bond formation.[52,53] This through-space antiferromagnetic contribution increases with incresasing SQ torsions and is therefore greatest in **2(SQZnL)$_2$**. As noted in the EPR section, the increased SQ torsions that give rise to large $|D|$ also result in increased antiferromagnetic coupling.

The exchange coupling parameters for those biradicals having a simple C═C Coupler (**2(SQZnL)$_2$**−**4(SQZnL)$_2$**, **6(SQZnL)$_2$**) can be correlated to the average SQ ring torsion angles (ϕ_{ave}) via a "Karplus−Conroy-type" relation,[64] eq 5:

$$J = A\cos^2(\phi_{av}) + B \qquad (5)$$

Equation 5 contains a $\cos^2\phi$ term because overlaps of 2p−π orbitals of the SQ groups with those of the ethene Coupler vary as the cosine of the torsion angles (ϕ) between the groups.[65] Due to the small number of data points, and for comparison to other systems, our primary concern is to keep eq 5 simple. To achieve this, we consider only a single trigonometric function, and we use an average of the two torsion angles. The data are displayed in Figure 7. The "fit" to eq 5 gives $A = 213$ cm^{-1} and $B = -44$ cm^{-1}. Given the simplicity of our model (eq 5), the *A*- and *B*-terms should be considered semiquantitative at best, as suggested by the thickness of the curve in Figure 7. Generally, the *A*-term should be a function of both the Coupler and the spin density in the spin-containing group, and in this case, the *B*-term should be proportional to the through-space antiferromagnetic interaction. In view of this, the ∼200 cm^{-1} range in *J*-values for **2(SQZnL)$_2$**−**4(SQZnL)$_2$** and **6(SQZnL)$_2$** is most likely greater than a corresponding breadth in related *m*-phenylene-type biradicals, due to the larger contribution of through-space contributions to J_{AF} in TMM-type biradicals, and the inherently stronger J_F provided by the ethene Coupler.[9,66] However, TMM-type biradicals, as assessed by our derivatives, can exhibit net ferromagnetic exchange coupling over a broad range of SQ ring torsions (≤ ∼60°).

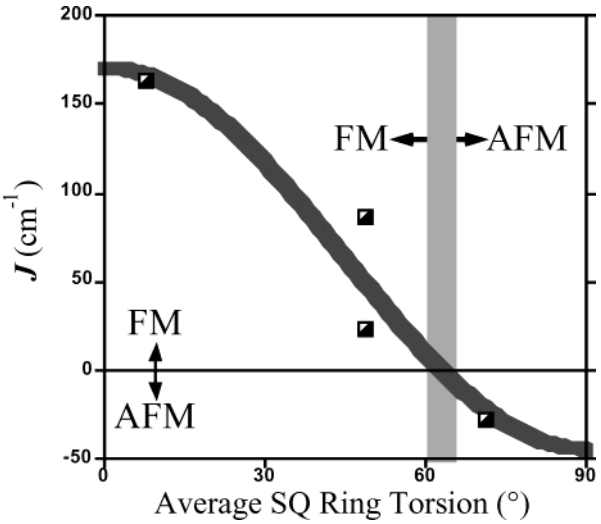

Figure 7. "Karplus−Conroy-type" relationship for electron spin exchange coupling in **2(SQZnL)$_2$**−**4(SQZnL)$_2$**, and **6(SQZnL)$_2$**.

The correlation of SQ ring torsion and exchange parameter is not perfect since the *J*-values for **3(SQZnL)$_2$** and **4(SQZnL)$_2$** differ by a factor of 3.6, yet the SQ ring torsions are nearly identical. We note however that the geometries of **3(SQZnL)$_2$** and **4(SQZnL)$_2$** are different: the former is asymmetric, while the latter has (crystallographic) C_2 symmetry. Clearly, there is more to the exchange coupling in this series than SQ ring torsion, as is the case for Karplus−Conroy NMR correlation.[64] Nevertheless, our series of biradicals shows a clear variation from strong ferromagnetic exchange coupling to moderate antiferromagnetic coupling as SQ ring torsion increases.

Correlation of Exchange Coupling in Biradical Complexes, and Mixed Valency in Quinone/Semiquinone Anions. The correlation of exchange coupling parameters with electron-transfer parameters is an area of intense, recent interest.[67−72] We feel that biradicals having exchange parameters that can be measured by magnetometry, and stability that permits X-ray crystallographic analysis are perhaps the optimal molecules to study the correlation of electron/energy transfer and exchange coupling.

In the electrochemistry section above, we suggested that $\Delta E_{1/2}$ (redox splitting) is a measure of stabilization of the mixed-valent

(61) There are other mechanisms by which these states can mix (e.g., hyperfine interactions), but these interactions are expected to be even weaker than vibronic mixing.
(62) This is similar to the case of cyclobutadiene, which distorts via a second-order Jahn−Teller distortion. The notable difference is that the latter is computed to be a singlet at all geometries when CI is included, see: Borden, W. T.; Davidson, E. R. *Acc. Chem. Res.* **1981**, *14*, 69−76.
(63) This asymmetry is a consequence of the enantiomerization mechanism, see: Kaftory, M.; Nugiel, D. A.; Biali, S. E.; Rappoport, Z. *J. Am. Chem. Soc.* **1989**, *111*, 8181−8191.
(64) Karplus, M. *J. Am. Chem. Soc.* **1963**, *85*, 2870−2871.
(65) Streitwieser, A., Jr. *Molecular Orbital Theory for Organic Chemists*; Wiley & Sons: New York, 1961; p 16.
(66) Wenthold, P. G.; Hu, J.; Squires, R. R.; Lineberger, W. C. *J. Am. Chem. Soc.* **1996**, *118*, 475−476.
(67) Weiss, E. A.; Ratner, M. A.; Wasielewski, M. R. *J. Phys. Chem. A* **2003**, *107*, 3639−3647.
(68) Lukas, A. S.; Bushard, P. J.; Weiss, E. A.; Wasielewski, M. R. *J. Am. Chem. Soc.* **2003**, *125*, 3921−3930.
(69) Weldon, B. T.; Wheeler, D. E.; Kirby, J. P.; McCusker, J. K. *Inorg. Chem.* **2001**, *40*, 6802−6812.
(70) Brunold, T. C.; Gamelin, D. R.; Solomon, E. I. *J. Am. Chem. Soc.* **2000**, *122*, 8511−8523.
(71) Teki, Y.; Ismagilov, R. F.; Nelsen, S. F. *Mol. Cryst. Liq. Crys. A* **1999**, *334*, 313−322.
(72) Nelsen, S. F.; Ismagilov, R. F.; Teki, Y. *J. Am. Chem. Soc.* **1998**, *120*, 2200−2201.

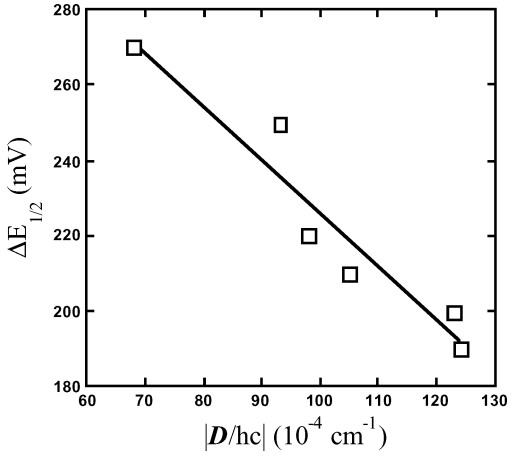

Figure 8. Correlation of $\Delta E_{1/2}$ for **2(Q)$_2$−7(Q)$_2$** and $|D/hc|$ for **2-(SQZnL)$_2$−7(SQZnL)$_2$**.

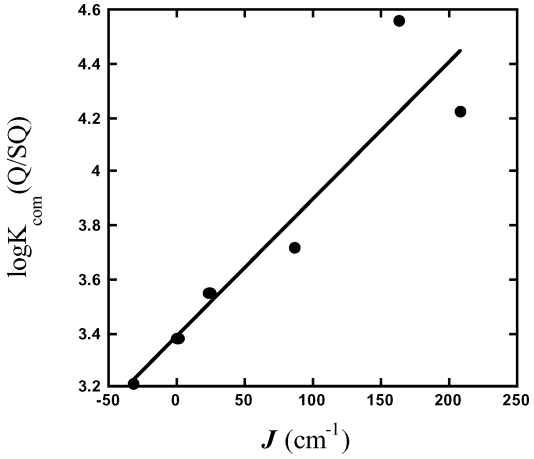

Figure 9. Correlation of log K_{com} for **2(Q)$_2$−7(Q)$_2$** and J for **2(SQZnL)$_2$−7(SQZnL)$_2$**.

Q−SQ species. However, there are several contributors to redox splitting, most importantly electrostatic effects.[73] Nevertheless, we feel that our observed *trend* in $\Delta E_{1/2}$ (and therefore K_{com}) does indeed reflect a trend in Coupler-modulated stabilization in the mixed-valent Q−SQ species. Our assertion is based upon the correlation displayed in Figure 8. As can be seen, the biradicals that give smaller *D*-values correspond to bis(Q) molecules that exhibit greater redox splitting (and therefore larger log K_{com}). If the redox splitting were due *solely* to electrostatic effects, it would be expected that the greatest redox splitting would correspond to a biradical with the greatest *D*-value since $|D|$ is inversely proportional to the cube of the interelectronic separation.[74] However, the exact opposite correlation is observed. However, as we mentioned in the electrochemistry section, redox splitting is also proportional to delocalization in mixed-valent species.[41] Therefore, the observed *trend* in $\Delta E_{1/2}$ reflects Coupler-modulated delocalization of the mixed-valent Q−SQ anions rather than simple electrostatics.

To correlate delocalization in mixed-valent Q−SQ molecules in our series with exchange coupling in the biradical forms, we begin by describing the electronic coupling matrix element for electron transfer in an isovalent biradical. This electronic coupling matrix element is given by the numerator of J_{AF} in eq 4 ($|V|^2$ is proportional to J_{AF}) and is re-cast in eq 6.

$$|V_{\text{isovalent}}|^2 = |2(\beta + l)|^2 \qquad (6)$$

As can be seen, electron transfer is most favorable when the magnetic orbitals have the same symmetry and therefore a nonzero transfer integral, β.[75] The necessary key connection between iso- and mixed-valent electronic coupling matrix elements was recently derived by Solomon et al. for dinuclear metal complexes.[70] These authors showed that the electronic coupling matrix elements for isovalent and mixed-valent forms are directly related ($|V_{\text{isovalent}}|^2 \approx 2|V_{\text{mixed-valent}}|^2$) and again $|V|^2$ is proportional to J_{AF}. For our purposes then, eq 6 is sufficient for the following qualitative arguments concerning the relation between exchange coupling in biradicals and electron transfer in mixed-valent forms of *cross-conjugated* molecules.

In our cross-conjugated, mixed-valent Q−SQ molecules, the electron transfer is between two orthogonal molecular orbitals (ϕ_1 and ϕ_2, Figure 6) for which the overlap integral is necessarily zero. Since the Wolfsberg−Helmholz approximation[65,76] relates β to the overlap integral, when the latter is zero β vanishes but l does not, and $|V_{\text{mixed-valent}}|^2 \approx 2l^2$. The integral l is the hybrid coulomb integral, and describes the electron−electron repulsion between the *overlap region* and each of the orbitals (vide supra).[37,57]

However, our observed trend in K_{com} (Table 5) as a measure of $|V_{\text{mixed-valent}}|^2$ suggests that $|V_{\text{mixed-valent}}|^2$ scales with biradical J_F, and *not* with J_{AF}, as seen graphically in Figure 9. It is the positive slope of this plot that indicates that log K_{com} is proportional to J_F, since J_F makes a positive contribution to J (see eq 4). This is initially counterintuitive but might be rationalized as follows. We hypothesize that the observed trend in K_{com} is a manifestation of the fact that the hybrid coulomb integral, l, scales with the exchange integral, k, since both integrals are proportional to the overlap density.[37,57] Thus, in cross-conjugated systems such as those described here, $|V_{\text{mixed-valent}}|^2$ scales with J_F, while in conjugated systems (or those with direct spatial overlap),[72] $|V_{\text{mixed-valent}}|^2$ is proportional to J_{AF}.

Interestingly, the through-space overlap that makes a large contribution to J_{AF} does not appear to provide an effective pathway for electron delocalization in the mixed-valent anions. This might be the result of different conformations for the biradical complexes and the mixed-valent anions so that the through-space overlap in the biradicals is smaller in the mixed-valent anions.

Conclusions

Our experimental results demonstrate that conformational *J*-modulation is strong in TMM-type biradicals. The breadth in *J*-values for the TMM-type biradicals is most likely greater than the corresponding breadth in related *m*-phenylene-type biradicals, although no magnetostructural study for a series of biradicals in the latter case has been reported.[21] The breadth in *J*-values for TMM-type biradicals studied herein is augmented by the larger contribution of through-space interaction to J_{AF} brought about by the close spatial proximity of the SQ groups. In fact, spin density close to the Coupler is critical, and the

(73) Ferrere, S.; Elliot, C. M. *Inorg. Chem.* **1995**, *34*, 5818−5824.
(74) Wertz, J. E.; Bolton, J. R. *Electron Spin Resonance*; Chapman and Hall: New York, 1986.
(75) For an example of symmetry-controlled energy transfer, see: Holten, D.; Bocian, D. F.; Lindsey, J. S. *Acc. Chem. Res.* **2002**, *35*, 57−69.
(76) Wolfsberg, M.; Helmholtz, L. *J. Chem. Phys.* **1952**, *20*, 837−843.

J-modulation in a similar isostructural series of bis(nitroxide) biradicals[26] is diminished compared to the present case. Nevertheless, TMM-type biradicals, as assessed by our bis(SQ) derivatives, can exhibit *net* ferromagnetic exchange coupling over a broad range of conformations ($0 \leq$ torsions $\leq$ ca. 60°). We also showed how energy matching of Coupler and SQ orbitals can enhance exchange coupling, as demonstrated by the fact that the conformation of **5(SQZnL)$_2$** is similar to that of **3(SQZnL)$_2$**, but *J* is nearly 1 order of magnitude greater for the former.

Our results also indicate that for the molecules studied, there is a qualitative correlation between the molecular conformations observed in crystal structures, and those adopted in frozen solution, as judged by EPR zero-field splitting parameters. This relationship results in similar *J*-values for solution and solid-state species. However, we note that linear EPR Curie plots only indicate that $J \geq 0$. A notable exception to the correlation between solution- and solid-state molecular conformation is the adamantyl-capped biradical, **3(SQZnL)$_2$**. The adamantyl group seems to impart interesting properties to TMM-type biradicals since we reported solvent-dependent conformational *J*-modulation for a bis(phenoxy) biradical analogue of **3(SQZnL)$_2$**[34] and hysteresis for a bis(nitroxide) derivative of **3(SQZnL)$_2$**.[54]

Finally, we correlate magnetic exchange coupling with Coupler-modulated delocalization within mixed-valent forms of our ligands. This is the first example of such a correlation within an isostructural series. Electron transfer in mixed-valent, cross-conjugated systems correlates with J_F, while theory indicates a correlation with J_{AF} for other systems. We propose that this correlation is the result of the fact that the hybrid coulomb integral, *l*, scales with the exchange integral, *k*. Thus, in cross-conjugated systems such as those described here, $|V_{\text{mixed-valent}}|^2$ scales with J_F, while in conjugated systems (or those with direct spatial overlap),[72] $|V_{\text{mixed-valent}}|^2$ is proportional to J_{AF}.

Experimental Section

General Experimental. Unless noted otherwise, reactions were carried out in oven-dried glassware under a nitrogen atmosphere. THF and toluene were distilled under argon from sodium benzophenone ketyl, and acetonitrile and methylene chloride were distilled from CaH_2 under argon. *tert*-Butyllithium (1.5 M in pentane) was used as received from Aldrich Chemical Co. Other chemicals were purchased from Aldrich Chemical Co. X-Band EPR spectroscopy and electrochemistry were performed as described previously.[77] NMR spectra were recorded at 300 MHz for ^{1}H NMR (referenced to TMS) and 75 MHz for ^{13}C NMR. Elemental analyses were performed by Atlantic Microlab, Inc., Norcross, GA. Mass spectrometry was carried out at the NC State University Mass Spectrometry Facility. Electronic absorption spectra were collected on a Shimadzu UV-3101PC scanning spectrophotometer. Other experimental details can be found in Supporting Information.

Synthesis. Catechols **3(CatH$_2$)$_2$**−**7(CatH$_2$)$_2$**[23,24] and their corresponding Zn^{II} complexes[22,27,78] were prepared as described previously, except for **4(SQZnL)$_2$** and **6(SQZnL)$_2$** which were prepared by a "comproportionation route" as described below for **2(SQZnL)$_2$**. Complex **6(SQZnL)$_2$** was prepared without the addition of KH. X-ray quality crystals for biradical complexes (except **6(SQZnL)$_2$**) were grown by layering methanol onto a methylene chloride solution of the biradical. Crystals of complex **6(SQZnL)$_2$** were grown in a glovebox using an analogous procedure, but replacing methanol with *n*-heptane. Carbinol **8** was prepared as previously described.[24]

5,5′-Di-*tert*-butyl-3,3′,4,4′-tetramethoxybenzophenone (9). A 100-mL flask containing CrO_3 (1.1 g, 11.0 mmol) was pump/purged three times with nitrogen. Pyridine (1.7 mL, 21 mmol) was added, and the mixture was dissolved in 20 mL of dry CH_2Cl_2. The solution was stirred for 0.5 h, and carbinol **8** (727.5 mg, 1.75 mmol) dissolved in 20 mL of CH_2Cl_2 was cannulated into the reaction. After stirring for 6 h, the reaction was quenched with 1 mL of 1 M NaOH, washed with brine, and dried over Na_2SO_4. Methanol was added to the resulting yellow oil to give a white solid (638 mg, 88%). ^{1}H NMR ($CDCl_3$) δ 7.39 (d, 2H, J = 2.1 Hz), 7.37 (d, 2H, J = 1.8 Hz), 3.96 (s, 6H), 3.92 (s, 6H), 1.38 (s, 18H). ^{13}C NMR δ 195.6, 153.3, 152.5, 142.7, 132.4, 122.7, 112.1, 60.7, 56.1, 35.4, 30.6. IR (film from CH_2Cl_2) ν (cm^{-1}): 2955.0, 1649.9, 1573.0, 1453.5, 1410.0, 1359.7, 1323.9, 1292.6, 1250.3, 1222.4, 1153.6, 1066.8, 1003.7, 762.3. HRMS (FAB): (*m*/*z*) $C_{25}H_{34}O_5$ $(M)^+$, Calcd 414.2406. Found 414.2393.

5,5′-Di-*tert*-butyl-3,3′,4,4′-tetramethoxy-thiabenzophenone (10). In a 100-mL flask benzophenone, **9**, (81.3 mg, 0.20 mmol), phosphorus pentasulfide (131.0 mg, 0.29 mmol), and sodium bicarbonate (100.8 mg, 1.20 mmol) were taken up in 10 mL of acetonitrile. The mixture was refluxed for 4 h during which time the color of the mixture turned blue. The mixture was cooled to 0 °C, quenched with saturated aqueous $NaHCO_3$, and washed twice with brine, and the blue solution was then dried over Na_2SO_4. The solvent was removed, and the blue solid was taken up in hot methanol and cooled to 0 °C to induce precipitation (44.6 mg, 0.10 mmol) in 51% yield. ^{1}H NMR ($CDCl_3$) δ 7.41 (d, 2H, J = 1.8 Hz), 7.25 (d, 2H, J = 2.1 Hz), 3.96 (s, 6H), 3.91 (s, 6H), 1.35 (s, 18H). ^{13}C NMR δ 235.2, 153.0, 152.9, 142.3, 142.0, 122.2, 113.5, 60.7, 56.0, 35.4, 30.6. IR (film from CH_2Cl_2) ν (cm^{-1}): 2998.4, 2956.1, 2866.9, 2832.6, 2600.7, 1995.7, 1582.8, 1567.3, 1478.5, 1450.4, 1405.5, 1359.7, 1314.4, 1288.8, 1249.4, 1205.7, 1151.3, 1073.7, 1060.9, 1002.9, 882.7, 860.0, 790.0, 704.5, 669.5. HRMS (FAB): (*m*/*z*) $C_{25}H_{34}O_4$ $(M + H)^+$ Calcd 414.2256. Found 414.2246. Anal. Calcd for $C_{25}H_{34}O_4$: C, 69.73; H, 7.96%. Found: C, 69.76; H, 7.88%.

11-[Bis-(3-*tert*-butyl-4,5-dimethoxyphenyl)-methylene]-bicyclo-[4.4.1]undecane (12). In a 50-mL flask thione **10** (401.2 mg, 0.93 mmol) was dissolved in 15 of mL THF. The diazo **11**, (182.2 mg, 0.94 mmol) was dissolved in 5 mL of THF and added dropwise to the stirring benzothione **10** solution. Bubbling and a white precipitate that quickly redissolved were observed. The blue solution was refluxed overnight. The solvent was removed and the remaining solid was taken up in 15 mL of toluene. Triphenylphosphine (502.3 mg, 1.92 mmol) was added, and the solution was refluxed for 2 days. Solvent was removed and the mixture purified by radial chromatography (gradient elution; petroleum ether to 10% ether/petroleum ether). The white solid was precipitated from petroleum ether, producing **12** (396.2 mg, 0.72 mmol) in 77% yield. ^{1}H NMR ($CDCl_3$) δ 6.78 (d, 2H J = 1.8 Hz), 6.62 (d, 2H J = 1.5 Hz), 3.84 (s, 6H), 3.81 (s, 6H), 2.91 (pent., 2H, J = 6.0 Hz), 1.68 (m, 4H), 1.55 (m, 12H), 1.36 (s, 18H). ^{13}C NMR δ 153.0, 146.6, 146.5, 142.7, 139.9, 139.4, 119.1, 111.0, 60.5, 56.0, 41.0, 35.2, 32.7, 30.9, 27.2. IR (film from CH_2Cl_2) ν(cm^{-1}): 2951.7, 2921.9, 2863.2, 1568.2, 1465.5, 1409.1, 1358.0, 1327.6, 1303.0, 1257.7, 1234.7, 1152.7, 1136.0, 1074.0, 1010.3, 937.1, 908.6, 878.7, 849.1, 780.0, 736.5, 704.4, 675.2. Anal. Calcd for $C_{36}H_{52}O_4$: C, 78.79; H, 9.55%. Found: C, 78.73; H, 9.76%.

11-[Bis-(3-*tert*-butyl-4,5-dihydroxyphenyl)-methylene]-bicyclo-[4.4.1]undecane (2(CatH$_2$)$_2$). A dry 50-mL flask containing tetramethoxyether **12** (153.6 mg, 0.28 mmol) and 30 mL of dry CH_2Cl_2 was pumped/purged three times with nitrogen. The solution was cooled to −78 °C. Boron tribromide (1.0 M in CH_2Cl_2, 5.6 mL, 5.6 mmol) was added dropwise, and the solution was stirred overnight (−78 °C to 25 °C). The solution was poured onto ice, washed with brine, and dried over Na_2SO_4. The crude catechol was used without further purification. ^{1}H NMR ($CDCl_3$) δ 6.72 (d, 2H, J = 1.5 Hz), 6.49 (d, 2H, J = 1.8 Hz), 5.43 (s, 2H), 4.75 (s, 2H), 2.97 (pent., 2H, J = 6 Hz), 1.67 (m, 4H), 1.53 (m, 12H) 1.39 (s, 18H). ^{13}C NMR δ 146.7, 142.7, 141.4, 138.9, 136.3, 136.2, 119.7, 113.4, 41.0, 34.8, 32.6, 29.9,

(77) Shultz, D. A.; Farmer, G. T. *J. Org. Chem.* **1998**, *63*, 6254−6257.
(78) Shultz, D. A.; Bodnar, S. H. *Inorg. Chem.* **1999**, *38*, 591−594.

27.2. IR (film from CH_2Cl_2) ν (cm^{-1}): 3519.7, 2921.2, 1590.2, 1483.7, 1415.4, 1362.6, 1289.6, 1237.6, 1049.9, 963.9, 862.7, 801.7, 737.7, 705.3, 663.9. HRMS (FAB): (*m*/*z*) $C_{32}H_{44}O_4$ $(M)^+$ Calcd 492.3240. Found 492.3238.

Di(5-*tert*-butyl-3,4-hydroxyphenyl)methylene-bicyclo[4.4.1]-undecane (2(Q)$_2$). A 50-mL flask containing **2(CatH$_2$)$_2$** (73.9 mg, 0.15 mmol) and 522 mg Fetizon's reagent was stirred with 25 mL of THF overnight. The mixture was filtered through SiO_2. Radial chromatography (CH_2Cl_2) yielded a yellow/green solid (65.9 mg, 90%). ^{1}H NMR ($CDCl_3$) δ 6.62 (d, 2H, J = 1.8 Hz), 6.21 (d, 2H J = 1.8 Hz), 3.07 (pent., 2H, J = 5.4 Hz), 1.76 (m, 4H), 1.55 (m, 18H), 1.27 (s, 18H). ^{13}C NMR δ 180.1, 179.3, 155.6, 152.9, 152.5, 136.0, 133.2, 127.2, 44.0, 35.9, 32.3, 28.4, 26.8. IR (film from CH_2Cl_2) ν (cm^{-1}): 2923.6, 1660.4, 1613.5, 1469.4, 1367.6, 1266.0, 1238.6, 910.4, 834.1, 805.4, 731.0. HRMS (FAB): (*m*/*z*) $C_{32}H_{40}O_4$ $(M + H)^+$ Calcd 489.3005. Found 489.3034.

2(SQZnL)$_2$. Inside a drybox, **2(CatH$_2$)$_2$** (27.9 mg, 0.057 mmol) and **2(Q)$_2$** (27.7 mg, 0.057 mmol) were combined in THF with excess KH and stirred for 15 min. In a separate vial KL[79] (162.2 mg, 0.25 mmol) and $Zn(ClO_4)_2$ $6H_2O$ (85.0 mg, 0.23 mmol) were stirred for 15 min. The solution of the **2(SQ)$_2$** and KH was filtered through a 0.2 μm syringe filter into the stirring KL and $Zn(ClO_4)_2 \cdot 6H_2O$. This solution was stirred for 15 min and was filtered through a 0.2 μm syringe filter, yielding the green biradical. IR (film from CH_2Cl_2) ν (cm^{-1}): 3423.1, 2923.3, 2525.6, 1552.3, 1616.4, 1445.2, 1360.0, 1182.6, 1064.3, 833.7, 787.5.

(79) Ruf, M.; Weis, K.; Vahrenkamp, H. *J. Chem. Soc., Chem. Commun.* **1994**, 135−136.

Crystallographic Structure Determinations. Pertinent information can be found in Supporting Information.

Magnetic Susceptibility Measurements. Magnetic susceptibilities were measured on a Quantum Design MPMS-XL7 SQUID magnetometer using an applied field of 1 T for Curie plots. Microcrystalline samples were loaded into the sample space of a Delrin sample holder, and mounted to the sample rod. Data were corrected for sample holder and molecular diamagnetism. The decrease in the χT data at low temperatures was accounted for with a Weiss correction, using the expression $\chi_{eff} = \chi/(1 - \vartheta\chi)$, where $\vartheta = 2zJ'_{inter}/(Ng^2\beta^2)$.[39] The origin of J'_{inter} may be zero-field splitting, intermolecular interaction, saturation effects, or some combination of all three.[40] The other terms have their usual meaning.[39] The data are plotted as χT vs T (Figure 2), except for **2(SQZnL)$_2$** which is also displayed as χ vs T in Figure 4.

Acknowledgment. This work is dedicated to Professor Dennis A. Dougherty. D.A.S. acknowledges the National Science Foundation (CHE-9910076; CHE-0091247, SQUID Magnetometer) for financial support and thanks the Camille and Henry Dreyfus Foundation for a Camille Dreyfus Teacher-Scholar Award. We thank Dr. Dadi Dai, Dr. Hyun-Joo Koo, Professor Mike Whangbo, and Professor Stefan Franzen for helpful discussions.

Supporting Information Available: Crystallographic data (in CIF format), electronic absorption spectra, EPR spectra for **3(SQZnL)$_2$**, and CV of **2(Q)$_2$** (PDF). This material is available free of charge via the Internet at http://pubs.acs.org.

JA0367849